

Producing Energy for Polar Stations from the Wind-Water Temperature Gradient

Hervé LeGoff, Uli F. Hasert

Laboratoire des Sciences du Génie Chimique-CNRS, France

Institut Français pour la Recherche et la Technologie Polaires (IFRTP), France

Antoine Guichard

Institute of Antarctic and Southern Ocean Studies (IASOS), University of Tasmania, Australia

Latitude Technologies, Australia

Abstract: We review the renewable resources available to produce heating and electrical power for polar stations in complement of conventional fossil fuels. For one Antarctic site (Dumont d'Urville) characterised by a standard meteorological year, we compare the energetic potential for solar, kinetic and thermal wind sources. The exergetic productions (i.e. usable heat or mechanical/electrical power) achieved by real and optimised systems (PVs, windgenerators, heat pumps, thermodynamic cycles) will be compared for the site.

The energy produced from the *thermal dipole* of the cold polar wind and the "warm" sea-, lake- or waste-water is described more precisely. We give a description of the principles of possible combined systems (heat transformers and thermodynamical cycles) and asses their efficiency computed with typical weather data for two stations: Dumont d'Urville, Adélie Land - Antarctica and Krenkel, Franz Josef Land - Russian Arctic. Two experiments currently carried out at both test sites consist in monitoring during two years the cooling power of the wind and in testing the heat exchangers designed to recover this kind of energy. The two experimental set-ups are described and first experimental results are presented.

Keywords: renewable, energy, environment, Antarctic, Arctic, absorption, heat pump, cold wind, thermal dipole

Erneuerbare Energieträger in polaren Gebieten

Zusammenfassung: Der Einsatz von Regenerativen Energieträgern, zusätzlich zu konventionellen Fossilen Energieträgern, wird im Hinblick auf deren Verfügbarkeit zur Wärmeabgewinnung als auch der Produktion Elektrischer Energie für Polarstationen untersucht. Anhand meteorologisch repräsentativer Daten wird das örtliche Energetische Potential von Solarer-, Kinetischer Wind- und Thermischer Windenergie einer Station in der Antarktis (Dumont D'Urville) miteinander verglichen. Die exergetischen Endprodukte, wie etwa nutzbare Wärme oder mechanische/elektrische Energie, resultierend aus realen, optimierten Umwandlungsprozessen (Photovoltaik, Windgeneratoren, Wärmepumpen, Thermodynamische Kreisprozesse) werden für selbigen Einsatz ebenfalls diskutiert.

Auf das Energieangebot, basierend auf dem *Thermischen Dipol*; kalter Polarwind - "warmes" Meer-, See- oder Abwasser; wird näher eingegangen. So zeigen wir dazu prinzipielle Möglichkeiten zum Einsatz von Wärmetransformatoren und Thermodynamischen Kreisprozessen. Deren Wirkungsgrade errechnen sich aus repräsentativen Wetterdaten zweier Polarstationen, Dumont D'Urville, Adélie Land - Antarktis und Krenkel, Franz Josef Land - Russische Arktis. Die gegenwärtig durchgeführten Experimente an selbigen Teststandorten, welche zur Ermittlung des Kühlpotentials von Polarwind und zum Test eigens konzipierter Wärmetauscher dienen, werden ebenfalls dargestellt, sowie erste Versuchsergebnisse vorgestellt.

Schlüsselworte: erneuerbar, Energie, Umwelt, Antarktis, Arktis, Absorption, Wärmepumpe, kalter Wind, thermischer Dipol

Production d'Énergie à partir du Gradient Thermique Air-Eau dans les Bases Polaires

Resumé: Nous analysons les possibilités d'emploi d'énergies renouvelables pour la production d'électricité et de chaleur, sur les bases polaires. Pour une base située en Antarctique (Dumont D'Urville), caractérisée par ses données météorologiques moyennes, nous comparons les potentiels énergétiques de trois sources d'énergie thermique du vent. Dans chaque cas nous calculons la production d'exergie correspondant à diverses machines réelles: capteurs photovoltaïques, aérogénérateurs, pompes à chaleur et machines thermodynamiques.

Nous décrivons plus particulièrement les techniques de production d'exergie à partir du *dipole thermique* constitué par le vent froid polaire et par l'eau "chaude" de la mer, d'un lac ou d'un rejet d'activité humaine. Les efficacités de ces machines sont calculées à partir des données météorologiques typiques de deux stations: Dumont d'Urville en Terre Adélie et Krenkel sur les îles François-Joseph en Arctique Russe. Des campagnes d'expérimentation sont en cours sur ces deux stations, afin d'y estimer, sur une période de deux ans, la puissance réfrigérante du vent et d'y tester des prototypes d'échangeurs de chaleur destinés à capter cette énergie. Les premiers résultats expérimentaux sont présentés.

Mots clés: renouvelable, énergie, environnement, Antarctique, Arctique, pompe à chaleur à absorption, vent froid, dipole thermique

1. Introduction

The need for better protection of the polar biosphere will lead to the development and introduction of new technologies making a better use of the renewable resources available in polar regions. Renewable systems based on PhotoVoltaics, Windgenerators or Heat Pumps could play an important role in the production of heat and electricity required by human activities in these regions,

complementing conventional fossil fuel based systems with both environmental and economical advantages.

We will describe and compare in this paper different ways of using such "clean" technologies, with a special emphasis on the production of energy from the thermal dipole existing between the "cold" polar wind and the "warm" sea-, lake- or waste-water.

2. The energy of the wind

The energy content E of one cubic meter of air (in J/m³ or Pa) relative to an arbitrary reference state "o" /1/, /2/ is expressed approximately with 4 terms:

$$\begin{aligned}
 E = & (P - P_0) \quad \{\text{I}\} \text{ Atm. Pressure Energy} \\
 & + 0.5 \cdot \rho \cdot (u^2 - u_0^2) \quad \{\text{II}\} \text{ Kinetic Energy} \\
 & + c_p \cdot \rho \cdot (T - T_0) \quad \{\text{III}\} \text{ Thermal Energy} \\
 & + L_v \cdot (C - C_0) \quad \{\text{IV}\} \text{ Drying Energy}
 \end{aligned} \quad (2.1)$$

where: P atmospheric pressure (Pa);
 (≈990 hPa along East Antarctic coast)
 ρ density of air (kg/m³);
 (≈1.3 kg/m³ at 990 hPa and -10°C)
 u wind velocity (m/s)
 c_p specific heat capacity (≈1003 J/kg/K)
 T temperature (°C or K)
 C concentration of vapour (kg/m³)
 L_v latent heat of vaporisation of water;
 (≈2470 kJ/kg at 20°C)

The gradients corresponding to each of these four energy components can be either time or space related depending on the choice of the reference state, but time gradients are not very practical to work with. Out of the four space gradients, two can be both consistent and practically recoverable: the velocity gradient (Δu between the air in motion and a fixed structure) and the temperature gradient (ΔT between the cold air and the 'warm' sea water).

For a so called "Typical" Year, the two corresponding energy components of equation 2.1 (II-kinetic & III-thermal) are calculated for 1m³ of air /8/. To obtain the power available from the wind, that is the amount of energy passing in one second through 1m² of vertical wind cross-section, we multiplied the wind energy by the wind speed. The resulting unit is then (W per m² of vertical wind cross-section), noted (W/m² vt), relatively consistent with the unit used for solar energy (W per m² of horizontal surface or W/m² hz). Both kinetic and thermal wind power are illustrated on Figure 2.1, along with solar power. It can be seen that potentially available thermal wind power is much higher than available kinetic or solar power.

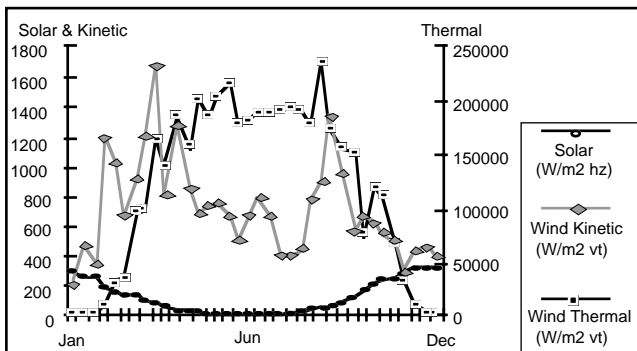


Figure 2.1: Typical seasonal variation of potentially available Wind Kinetic, Wind Thermal & Solar Power (Dumont d'Urville, based on 1986-89 data)

2.1 The velocity gradient

The velocity gradient of the wind can be used to drive a wind turbine. A realistic efficiency for a basic and reliable two bladed horizontal axis turbine producing electricity is: $\Phi_{\text{WindTurbine}} = 25\%$. This is the proportion of the wind kinetic power which will be transformed by the turbine into electrical power.

2.2 The temperature gradient

At Franz Josef Land and Dumont d'Urville (our two test sites), and at other Antarctic coastal stations, the sea water is at a fairly constant temperature of about $T_0 \cong -1.8^\circ\text{C}$, close to its freezing point. It provides, during the polar winter, a consistent temperature gradient between the air and this 'warm' sea (the "thermal dipole").

There will be two possible ways to use the resulting wind thermal energy component (II):

a) heat generation

Heating buildings with water at 70°C can be achieved with a heat transformer (normally made of a multistage absorption heat pump) using the wind-sea water thermal gradient for the separation process (discussed later, see Figure 2.2 and upper part of Figure 2.3.

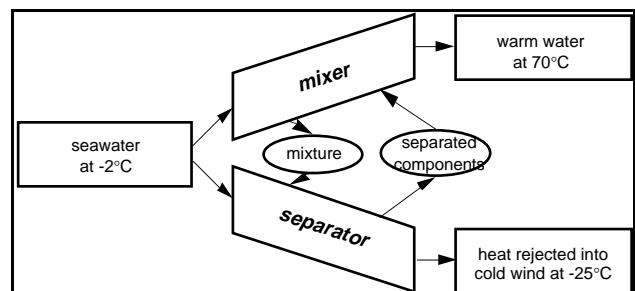


Figure 2.2: Principles of the heat transformer

b) electricity generation

The same thermal gradient can drive a basic Rankine cycle machine (vapour turbine), which has proved feasible in the OTEC (Ocean Thermal Energy Conversion) projects using the 20°C gradient between tropical ocean surface water and deep water (thermomechanical machines) /3/. The vapour turbine can then drive an alternator to produce electricity. More sophisticated cycles combining heat pumps and turbines can later improve the global efficiency (with the possibility of energy storage), see Figure 2.2 and lower part of Figure 2.3.

We will base our output estimations on the thermomechanical machines for proper comparison with photovoltaics and wind turbines, which also provide electrical outputs. However, It must be noted that heat pumps would produce heat with better efficiencies and should be well suited to space heating in the stations as their production capabilities would be coupled with the heating demands: "The stronger and colder the wind, the more powerful the heat pump!"

3. Thermomechanical Machines

The temperature gradient that typically exists between sea water and air provides a potential source of renewable energy. Thermomechanical machines convert the thermal difference to mechanical power which in turn can be converted into electrical power via an alternator (see Figures 2.2 and 2.3).

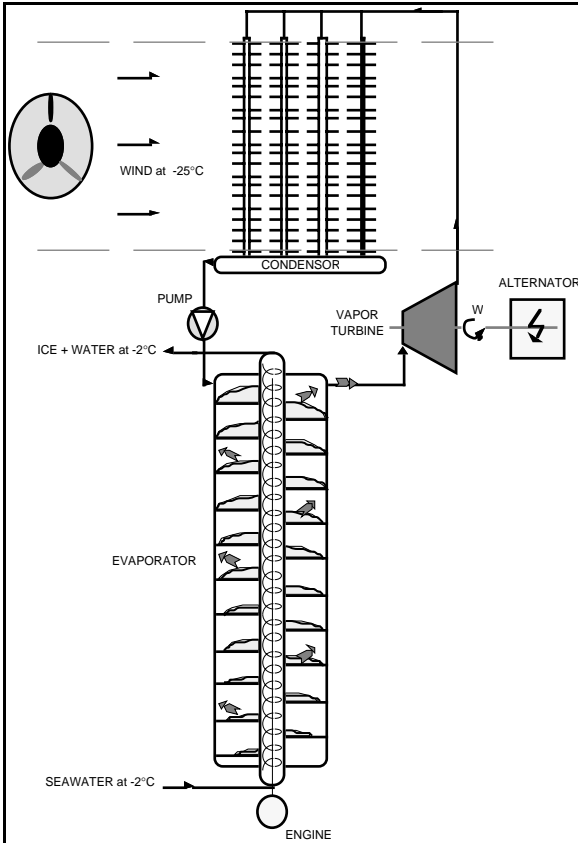


Figure 2.2: Thermomechanical machine working between the warm sea water and the cold wind

The thermomechanical machines are inspired from OTEC machines. Their efficiency in converting Thermal to Mechanical power can be roughly expressed as /8/:

$$\phi_{TM} = \phi_{Carnot} \cdot \phi_{real} \cdot \phi_{usable} \quad (3.1)$$

where: ϕ_{Carnot} "limit" Carnot efficiency of the cycle
 ϕ_{real} proportion of ϕ_{Carnot} practically attainable
 ϕ_{Usable} proportion of usable temperature gradient, (temperature drop ΔT_{usable} of the air when passing through the exchanger)

With temperatures given in °Kelvin, the Carnot efficiency of the cycle is:

$$\phi_{Carnot} = \frac{\left(\Delta T - \frac{\Delta T_{usable}}{2} \right)}{T_0} \quad (3.2)$$

Following our first experiments, detailed further in this paper, values put forward for both ϕ_{real} and ϕ_{Usable} are of the order of 25%. They have to be further confirmed and refined by in-situ trials of prototypes.

A typical efficiency for an alternator converting Mechanical Power into Electrical Power is $\phi_{ME} = 80\%$.

Then the final Thermal to Electricity efficiency ϕ_{TE} is:

$$\phi_{TE} = \phi_{TM} \cdot \phi_{ME} \quad (3.3)$$

which should be in the order of: $\phi_{TE} = 0.05 \cdot \phi_{Carnot}$.

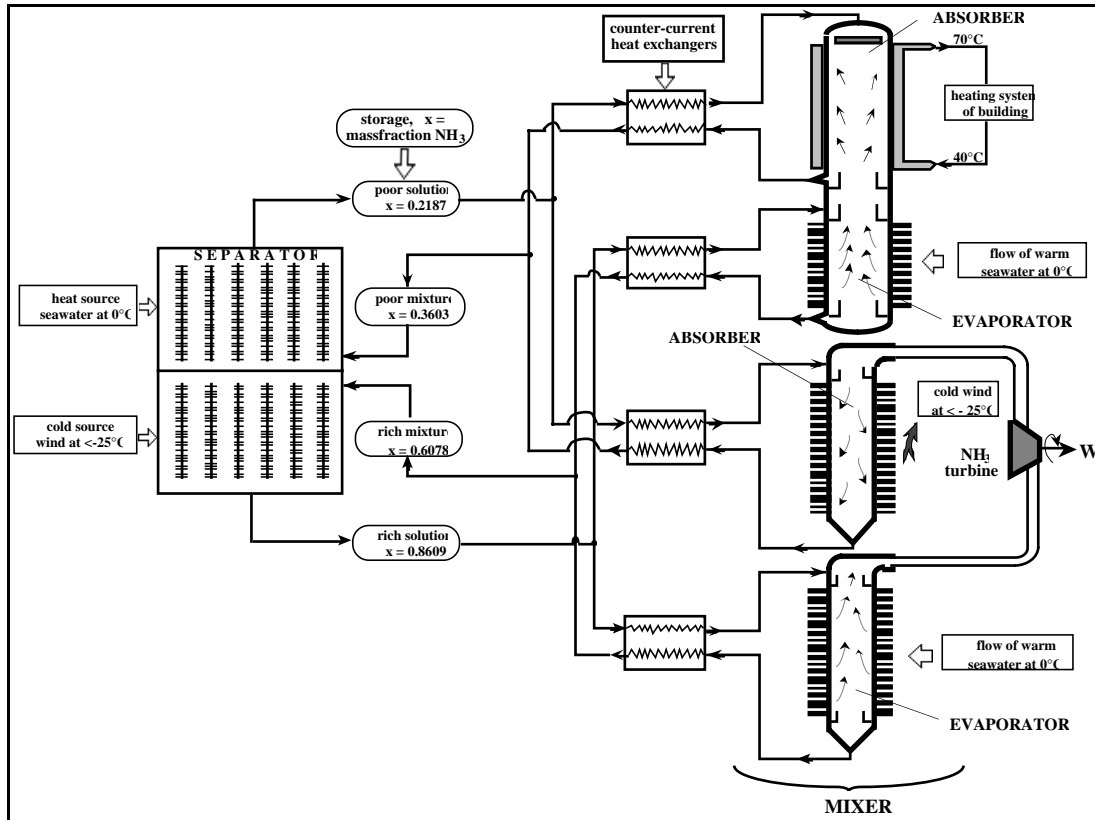


Figure 2.3: NH₃-H₂O system using the dipole polar wind/sea water to generate heat and power

This efficiency is used to calculate the electrical power recoverable from the wind by an electro-mechanical machine. Electrical power recoverable throughout the Typical Year (Wind Kinetic, Wind Thermal and Solar) is illustrated on Figure 3.1 and Table 3.1.

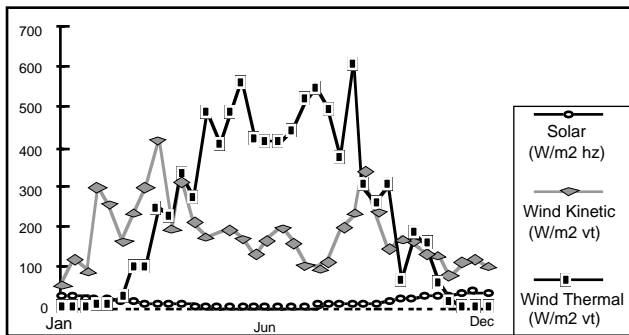


Figure 3.1: Typical seasonal variation of Recoverable Electrical Power

(Dumont d'Urville, based on 1986-89 data)

	Yearly Average	Highest Decade	Lowest decades
Solar	11.7	32.9 dec 1-10	< 2.0 may 1-aug 20
Wind Kinetic	181.4	422.4 mar 21-31	56.9 jan 1-10
Wind Thermal	246.1	616.9 sep 1-10	< 2.0 dec 1-feb 10

Table 3.1: Recoverable Electrical Power (W/m²), Extremes and Averages of Typical Year.

(Dumont d'Urville, based on 1986-89 data)

These calculations indicate that if good overall practical efficiencies can be obtained, the method could provide, for the same cross section of wind used, more

energy than rotating machines which exploit the kinetic energy of the wind. The potential for energy production is less constant throughout the year than from wind kinetics, but has the advantage of providing most energy in winter when heating requirements are greatest. The strong point is that this method involves far lighter and more reliable machines as no moving parts are exposed.

4. Multi-effect absorption cycles

Multi-effect absorption heat pump cycles provide far superior heating performances than single-stage cycles /4/. There are many possible combinations for multi-effect absorption cycles, but all of them can be decomposed into elementary building blocks which are single-stage absorption cycles with well known performances. The principle of an elementary absorption cycle is always the same, see figure 3.1:

One part of the low temperature heat source (sea water) is degraded to a low temperature in separating a binary mixture. The complementary part is upgraded to a high temperature in remixing the two constituents.

Each working pair has its own restricting conditions, as for example a special field of temperature, concentration, pressure... We used in our simulated absorption cycle the well known binary mixture ammonia-water.

The separation unit of the heat transformer uses a process called "fractional quasi isothermal distillation" /5/. Herein the difference between the heat sink and the heat source is very small (about 10K) and the pressure varies from one stage to the other (from 0.1 to 1.427 bar). The

separation is realised in 7 stages, to produce a rich solution $x_{RS}=0.7703$ (mass fraction of NH_3) and a poor solution of $x_{PS}=0.2187$, starting from a rich mixture of $x_{RM}=0.5767$ and a poor mixture $x_{PM}=0.3603$.

The mixing is done in a two stage mixer at different pressure ($p_{1M}=1.427\text{bar}$, $p_{2M}=3.25\text{bar}$), coupled in thermal series and in material parallel, see Figure 4.1 /6/ The temperatures inside the cycle are estimated to:

$T_{ab}=70^\circ\text{C}$ input temperature for the heating system of buildings
 $T_{water}=T_{ev}=T_{des}=-2^\circ\text{C}$ sea water, evaporation and desorption temperature
 $T_{wind}=T_{ev}=T_{con}=-25^\circ\text{C}$ wind, evaporation and reference temperature

As an example, we looked at an absorption heat transformer with a nominal power at the absorber of $Q_{ab}=1\text{kW}$. Under these conditions the separator needs a heating (desorption) and cooling (condensation) power of $Q_{des}=Q_{con}=9.9\text{kW}$. The heating power for the mixer (evaporation) is $Q_{ev}=0.45\text{kW}$. This finally results in a performance coefficient for the whole cycle of:

$$COP = \frac{Q_{ab}}{Q_{ev} + Q_{des} + W_p} = 6.51\% \quad (4.1)$$

where: Q_{ab} absorption heat (kW)
 Q_{ev} evaporation heat (kW)
 Q_{des} desorption heat (kW)
 W_p electrical energy for the solution pumps, (estimated to $W_p=5\text{kW}$)

The low COP of this heat transformer is due to the high demand of heat at 0°C . The advantage of such systems is the possibility to produce usable heat from a very low heat source temperature ($T_{water}=0^\circ\text{C}$). When we look with a financial cost view at equation 5, where the COP is defined as the ratio between the useable, produced energy to the costly consumed energy, it can be seen that for a "gratis" heat source, and without taking into account the operation cost, the denominator gets "zero" and so the COP gets "infinitely big".

To compare our results from the heat transformer with the estimation made earlier for Thermal to Electrical power conversion, we can estimate for a pure Thermal to Heating power efficiency the COP of 6.51%, which will be superior to the $\phi_{TM} = 0.05 \cdot \phi_{carnot}$ estimated for the Thermomechanical machine.

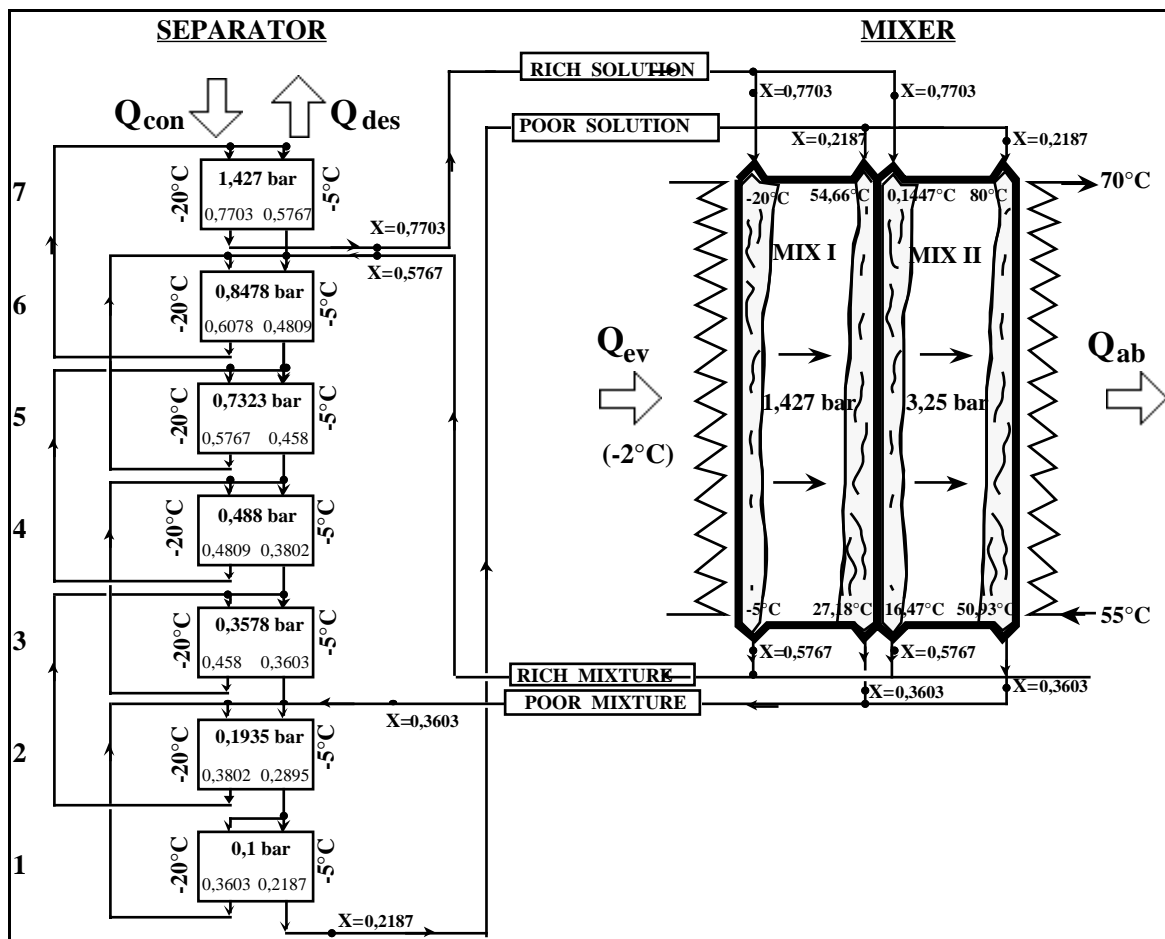


Figure 4.1: Ammonia-water multi-effect absorption cycle

5. Description of the "cold wind fluxmeter"

On the wind side, the design of the heat exchanger in the absorption cycle requires a good knowledge of the heat transfer characteristics between a heated wall and the unstationary cold wind carrying snow and/or ice.

Heat transfer effects usually used in air-cooled refrigeration cycles are either natural or artificially forced convection. But the use in forced convection of natural wind, with its uncertain and transitory conditions, is not well known. Then, in the experimental stage, we try to evaluate under real meteorological conditions the heat transfer between vertical tubes internally heated (electrically) and the cold wind. There are several unknown parameters, which directed the design of our installations at the test sites: the unique, rough meteorological conditions (extreme winds, low temperatures), the possible presence of snow and the satisfactory operation of the heat exchanger under a very small temperature gradient.

An experimental device, called "cold wind fluxmeter", was designed and built at the LSGC in Nancy, Figure 5.1 shows the fluxmeter [7].

The cold wind fluxmeter consists of two vertical, cylindrical, tubes: one smooth tube, with a well-known tube-wind heat transfer and one tube with external, annular fins, for the testing of snow effects and to increase the heat transfer by increasing the effective surface area of the tube. The internal electrical resistance is generating the thermal gradient for heat flux transfer.

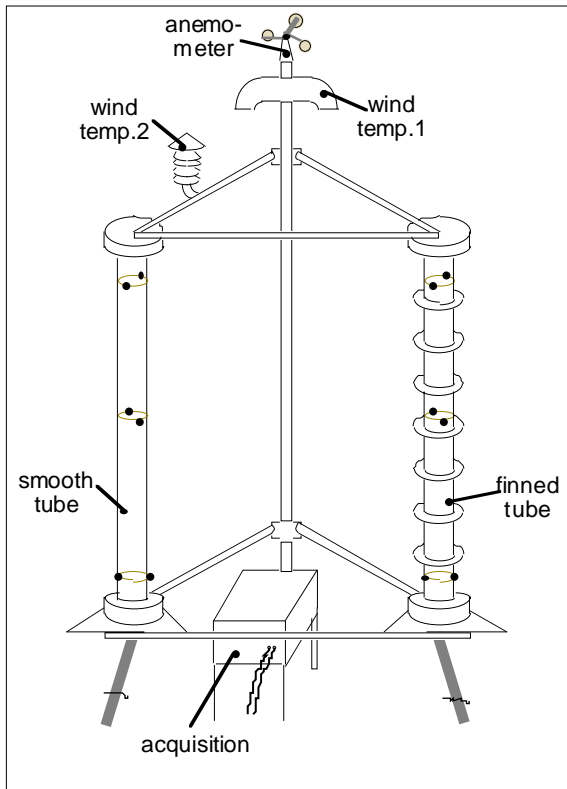


Figure 5.1: The cold wind fluxmeter

Tube surface temperature, wind temperature and speed are measured and recorded continuously by an automatic data acquisition system. After some preliminary testing in the French Alps, the first fluxmeter was installed in the 1993 northern summer at the meteorological station of Krenkel, Franz Joseph Land, in the Russian Arctic, and the second in January'94 at the French Antarctic Station Dumont d'Urville.

Meteorological characteristics of these two locations (Krenkel, Arctic, and Dumont d'Urville, Antarctic) are quite different. The average temperature at Krenkel during the 4.5 months of polar night is around -30°C . At Dumont d'Urville there is no polar night and the temperatures are not as low, but there are very strong catabatic winds with recorded speeds up to 90 m/s. The aggregation of results obtained at those two different locations will improve the reliability of our conclusions and expand their scope.

The next step towards a real working unit will be taken in January 1995 with the installation of a bundle of tubes as heat exchanger. It will represent the real condenser planned for the final installation and will provide more detailed information on the wind refrigeration power practically recoverable.

6. Details on the heat transfer

The equation characterising the heat transfer between the external tube surface and the cold wind is:

$$P_{\text{elec}} = h \cdot A \cdot (T_d - T_a) \quad [\text{W}] \quad (6.1)$$

where:

P_{elec} heating power (W)

h heat transfer coefficient ($\text{W}/\text{m}^2\text{K}$)

A heat exchange surface (m^2)

T_d average tube surface temperature (K)

T_a wind temperature (K)

The heating power P_{elec} is known, the tube surface temperature T_d and the wind temperature T_a are measured with different thermocouples, and the only unknown parameter is the heat transfer coefficient h_c . This coefficient depends on the velocity of the wind. By measuring the wind velocity u and evaluating the constants K and n (corresponding to the wind flow conditions), we can determine h , expressed by the following equation:

$$h = K \cdot u^n \quad \left[\frac{\text{W}}{\text{m}^2 \text{K}} \right] \quad (6.2)$$

The temperature difference ΔT between the wind and the tube should be kept approximately constant at 10K, which will represent the real working conditions of the heat exchanger in the absorption cycle. To hold this temperature difference, the heating power P_{elec} is regulated as a function of meteorological conditions, especially wind velocity (see eq. 6.1 and 6.2). Each determination of the heat transfer coefficient h_c must be made for a stable period, this means for a specific wind velocity. Therefore, we try to get a pseudo-permanent period by estimating stages for the regulation of the heating power P_{elec} in function of the wind velocity u . This is done by the application of a certain hysteresis to avoid an oscillation of the electrical power.

A fully automatic data acquisition is undertaken via a chain of electronic modules and a PC. Each data channel is read every 2 seconds and averaged every 5 minutes for recording by the PC, which is also piloting the electrical heating of the tubes.

6.1 Smooth tube

The heat transfer of a smooth tube has been well studied, and Hilpert /9/ gives the following empirical correlation:

$$Nu = C \cdot Re^n \cdot Pr^{1/3} \quad (6.3)$$

with: Nu Nusselt number, representing the dimensionless temperature gradient at the surface and defined as:

$$Nu = \frac{h \cdot d_h}{\lambda} \quad (6.4)$$

Re Reynolds number, representing the ratio of the inertia and viscous forces, defined as:

$$Re = \frac{u \cdot d_h}{\nu} \quad (6.5)$$

Pr Prandtl number, representing the ratio of the momentum and mass diffusivities, defined as:

$$Pr = \frac{\mu \cdot c_p}{\lambda} \quad (6.6)$$

C and n are constant for different flow conditions. Values are listed in Table 6.1. The noted velocity ranges couldn't be measured by our installation, so in our case only wind velocity up from 1 m/s is recorded. All thermodynamical properties are evaluated at the air temperature.

Re	u (m/s)	C	n
0-4	0-0.001	0.989	0.330
4-40	0.001 -0.01	0.911	0.385
40-4000	0.01-1	0.683	0.466
4000-40000	1-10	0.193	0.618
40000-400000	10-100	0.027	0.805

Table 6.1: Constants for a circular cylinder in cross flow.

Transforming the equations (6.3-6.6) we will get an expression for the heat transfer coefficient h, similar to equation 2:

$$h = \left(\frac{c_p \cdot \lambda}{\nu^n} \cdot d_h^{n-1} \cdot Pr^{1/3} \right) \cdot u^n \quad (6.7)$$

where: h coefficient of heat transfer by convection in (W/m²K)

c_p specific heat at constant pressure in (J/kg K)

λ thermal conductivity in (W/m K)

ν kinematic viscosity in (m²/s)

d_h characteristic length, hydraulic diameter in (m)

u wind velocity in (m/s)

μ viscosity in (kg/s m)

Using the correlation after Hilpert, and for a reference temperature of the air T=0°C, we should get for the heat transfer coefficient of our smooth tube the value: h=13.2 u^{0.62}. Values of h estimated from our first experiments will be detailed further in this paper.

We have to take into account other heat transfer effects, such as the solar radiation part, the infrared radiation back to the sky and the floor or a wet air circumstance, which will have an influence on equation 6.7, in order to obtain a corrected value for h called from now on h_c.

$$h_c = \frac{P_s \cdot \alpha_d}{A(T_d - T_a)} + \frac{P_{elec}}{A(T_d - T_a)} + \frac{\sigma \cdot \epsilon_d}{2(T_d - T_a)} \left[(T_d^4 - T_{sky}^4) + (T_d^4 - T_a^4) \right] \quad (6.8)$$

solar radiation electric heating infrared radiation (sky/floor)

where: P_s solar radiation in (W/m²)
α_d absorptivity of the tube
σ=5.67 10⁻⁸ (W/m²K⁴)
Stefan-Boltzmann constant
ε_d emissivity of the tube
T_{sky} sky temperature in (K)

6.2 Finned tube

For the tube with external, annular fins, built with the same general dimensions (external diameter and length), we have to apply the theory of the fin efficiency η_f. The definition of the fin efficiency is the ratio of the transferred heat flux Q_f to the maximal possible (if the entire fin surface were at the base temperature) transferred heat flux Q_{fmax}:

$$\eta_f = \frac{Q_f}{Q_{fmax}} \quad (6.9)$$

The fin efficiency is obtained after Schmidt from /10/:

$$\eta_f = \frac{\tanh(m \cdot r_d \cdot \varphi)}{m \cdot r_d \cdot \varphi} \quad (6.10)$$

$$\text{with: } \varphi = \left(\frac{r_{fin}}{r_d} - 1 \right) \left[1 + 0.35 \cdot \ln \left(\frac{r_{fin}}{r_d} \right) \right] \quad (6.11)$$

$$\text{and } m = \sqrt{\frac{4h_c}{\lambda_{\text{fin}} \cdot \delta}} \quad (6.12)$$

where: r_d external tube radius in (m)
 r_{fin} external fin radius in (m)
 δ thickness of the fin in (m)
 λ_{fin} thermal fin conductivity in (W/m K)

With the fins in place, the heat transfer rate is:

$$Q_{\text{tot}} = Q_f + Q_b \quad (6.13)$$

where: Q_f heat transferred by the fins (W)
 Q_b heat transferred by the basic smooth tube (W)

From equation 6.9, the fin heat transfer rate is:

$$Q_f = N \cdot \eta_f \cdot Q_{f_{\text{max}}} = N \cdot \eta_f \cdot h_c \cdot \Delta T_f \cdot A_{\text{fin}} \quad (6.14)$$

where: N number of fins
 A_{fin} fins surface (m²)

Heat transfer from the exposed surface is:

$$Q_b = h_c \cdot \Delta T_f \cdot A_b \quad (6.15)$$

where: A_b basic smooth tube surface (m²)

We emphasize that the heat transfer coefficient for the finned tube is referred to A_b the basic smooth tube surface.

For comparison of the finned tube and the smooth tube, we defined a factor F_b as:

$$F_b = \frac{Q_{\text{tot}}}{P_{\text{elec}}} \quad (6.16)$$

where P_{elec} is calculated with the same difference of temperature as for the smooth tube ($\Delta T=10\text{K}$). But as the heat transfer of the finned tube increased we took $\Delta T_f=5\text{K}$. The results of this comparison are shown in table 6.2:

u (m/s)	1	5	10	15	20	25	30
$h_c(\text{W/m}^2\text{K})$	13.2	35	55	70	84	97	108
P_{elec}	11	30	46	60	71	82	92
Q_{tot}	63	170	261	334	398	456	509
F_b	5.7	5.6	5.6	5.6	5.6	5.5	5.5

Table 6.2: Comparison of the finned and smooth tubes

Finally it shows that the finned tube should dissipate a power about 5 times higher than that of the smooth tube: $h_{\text{fin}} \cong 5 \cdot h_{\text{smooth}}$ or $h_2 \cong 5 \cdot h_1$.

But we will show in chapter 7 that it was not true for some of our experimental results.

7. First experimental results

After the first experimental results from the test sites, we can distinguish 3 different zones of working conditions, presented in figure 7.1:

A) $u < 5 \frac{\text{m}}{\text{s}} \Leftrightarrow \text{Re} < 20000$:

In this first zone, the heat transfer coefficient h_{biblio} (after Hilpert) doesn't provide satisfying results, as the calculated coefficient h_{1c} for the smooth tube is inferior to the expected values. We can explain it with the strong influence of the radiative heat exchanges compared to the convective exchanges. This influence is stronger on the smooth tube as on the finned tube. The ratio between h_2/h_1 raises up to 6.

B) $5 \leq u < 10 \frac{\text{m}}{\text{s}} \Leftrightarrow 20000 \leq \text{Re} < 40000$:

The radiative part represents in this area 15-20% of the heat transferred due to the convection during the day and up to 30% during the night. This will always provoke a difference between the h_{biblio} and the calculated coefficient h_{1c} for the smooth tube, but not as important as for wind velocity around 5 m/s. The ratio between h_2/h_1 is about 5 as seen before.

C) $u \geq 10 \frac{\text{m}}{\text{s}} \Leftrightarrow \text{Re} \geq 40000$:

When wind velocity exceeds 10 m/s ($u \geq 10 \frac{\text{m}}{\text{s}}$), the influence of the radiative heat exchange gets small compared to convective exchange. The influence on the heat transfer coefficient h is less than 13%, which means that it will be within the uncertainty of the measurement and calculation of h . We can see clearly on figure 7.1 that for such high wind velocities, the lines for h_{biblio} and h_{1c} are closed parallels, and that the points of measurement are grouped close to the lines of linear regression (h_{1c} and h_{2c}), which means that in this area our estimations seem coherent. The ratio between h_2/h_1 is around 4.

As the average wind velocity at Dumont d'Urville is from 8 to 20 m/s, our installation is well adapted to this test site. But on the northern test site on Franz Joseph Land, the average wind velocity is not as high, which will result in greater uncertainties about the data.

Production of energy from the wind-water temperature gradient is under the direct influence of the temperature difference ΔT , but also of the wind velocity, as for machines using the sole kinetic component of wind energy.

As a first result for the overall heat transfer coefficient h_c concerning the two tubes, we will give the following expressions (a) and (b), functions of the velocity of the wind;

a) heat transfer coefficient of the smooth tube:

$$h_{1c} = 0.053 \cdot \text{Re}^{0.655} \left[\frac{\text{W}}{\text{m}^2 \cdot \text{K}} \right] \\ = 12.123 \cdot u^{0.655}$$

b) heat transfer coefficient of the finned tube:

$$h_{2c} = 0.969 \cdot \text{Re}^{0.515} \left[\frac{\text{W}}{\text{m}^2 \cdot \text{K}} \right] \\ = 69.404 \cdot u^{0.515}$$

These results lead to the overall efficiency mentioned earlier:

$$\phi_{TE} = 0.05 \cdot \phi_{Carnot}$$

These first estimations of possible heat transfer coefficient for a single cylindrical tube (smooth or finned) will be further refined in the future with the access to other test sites and to more detailed meteorological data.

Meteorological data from our Russian test site, Krenkel, will be further processed in cooperation with

scientists from the Norwegian Polar Institute while data from Dumont d'Urville will be directly processed by our team. A similar evaluation will be undertaken for different Northern Canadian sites by our cooperating partners at the Ecole Polytechnique, Montreal.

The evaluation of those long term weather data shall give us information about the energy resource potential of the sites and thus the possibility of operating complete heat pump systems at those sites.

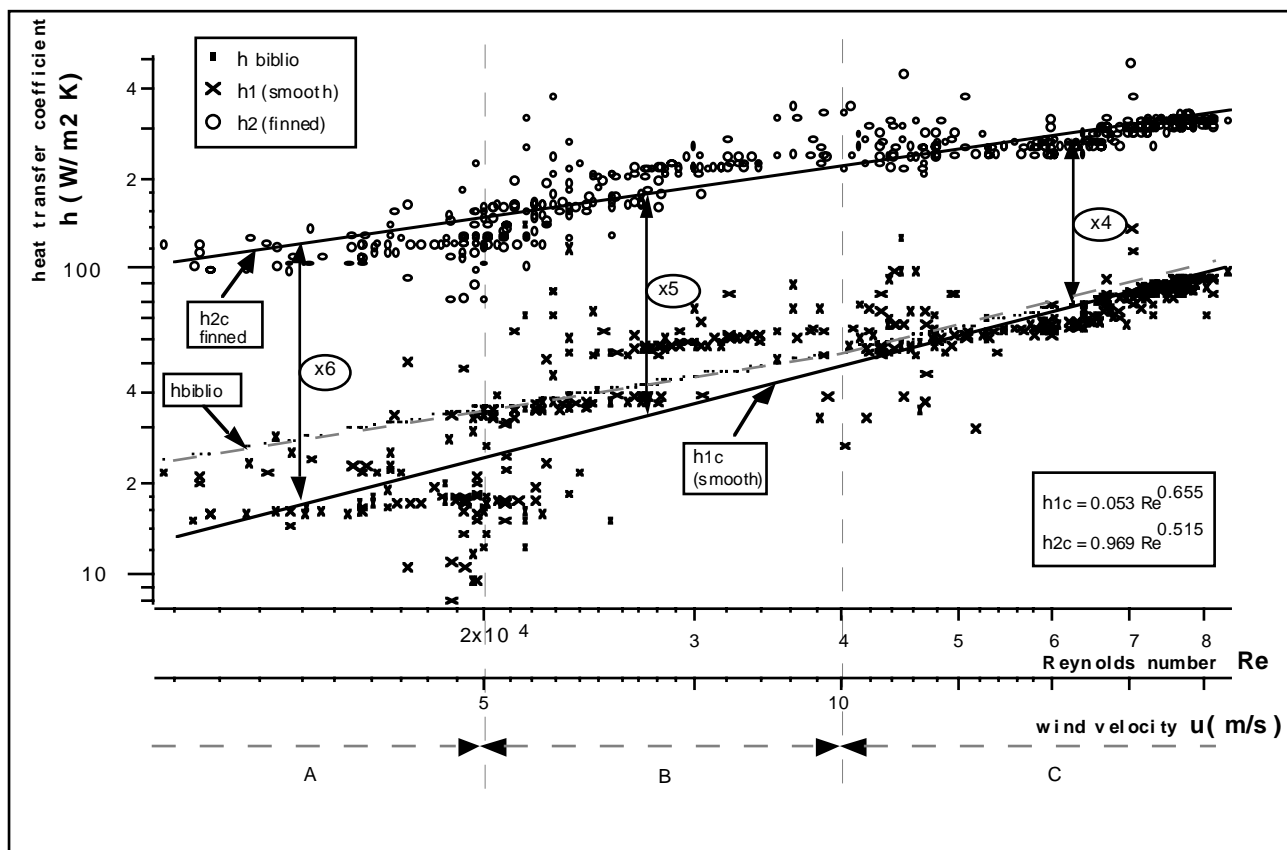


Figure 7.1: First experimental results of the test site (DDU January 1994)

5. Conclusions

The provision of energy to polar stations using conventional fossil fuels is costly, difficult logistically and has significant environmental impacts. This makes any improvement of energy systems at the stations far more cost-effective than at most other places on earth.

Improving the energy systems is, and has always been, an everyday job for the technical staff of the agencies operating the stations. This staff has valuable experience and great motivation to pursue the development and implementation of new solutions.

Researching and implementing clean and efficient alternative energy systems in polar regions could have an invaluable role in perfecting and demonstrating promising systems to be used around the world. Among such systems, thermal machines could play an important and valuable role. And the thermal dipole of the cold polar wind

and the "warm" sea water could bear more potential if using as heat source lake-water or waste water with temperatures higher than sea water. But the use of a waste water, will mean that we have to give up our idea of the "real" renewable energy resource...

Acknowledgements

The authors gratefully acknowledge the assistance of the Institut Français pour la Recherche et la Technologie Polaires (IFRTP), the Australian Antarctic Division, the Institute of Antarctic and Southern Ocean Studies at the University of Tasmania and the French Ministère de la Recherche. Thanks to Prof. P. LeGoff for reviewing this document, and all others making our study possible.

Bibliography

- /1/ P. LE GOFF
Exploitation d'une nouvelle forme de l'énergie solaire :
la froideur du vent, Entropie, n° 107-108 (1982)
- /2/ H. LE GOFF, B. SCHWARZER, P. LE GOFF
Utilisation des énergies renouvelables en milieu
polaire, Congrès de Génie des Procédés, Grenoble-
France, (09/1993)
- /3/ A. LAVI
Ocean Thermal Energy Conversion the French
Programme, a pilot electric power plant for French
Polynesia 1978-82 : a general introduction
Energy, vol 5, (1985)
- /4/ F. ZIEGLER, R. KAHN, F. SUMMERER, G. ALEFELD
Multi-effect absorption chillers, Int.J.Refrig. (1993),
Vol 16, No 5, pp.301-311
- /5/ B. SCHWARZER, S. DE OLIVEIRA JR, P. LE GOFF
An absorption heat transformer for space heating
driven by the thermal energy of the wind
Communication to IECEC-Boston, (1991)
- /6/ U. HASERT
Thermische Energie von kaltem Polarwind,
Unpublished Thesis, "Diplomarbeit", LSGC und
Universität Stuttgart, (09/1993)
- /7/ J. VIVANT
Mise au point d'un fluxmètre à énergie du vent froid,
Unpublished Thesis,, "Diplôme d'étude approfondie-
DEA", LSGC-INPL, Nancy, (10/1993)
- /8/ A. GUICHARD, J. STEEL
Alternative energy options for Antarctic stations:
Investing for the future, Conference IDEEA Two,
Montréal-Québec, Canada, (10/1993),
- /9/ R. HILPERT
Forsch. Geb. Ingenieurwesen N°4, p. 215, (1933)
- /10/ T.E.SCHMIDT
Die Wärmeleistung von berippten Oberflächen
Abhandlung. d. Deutschen Kältetechnischen Vereins,
N° 4, (1950)

This paper was presented at the:
" Sixth Symposium on Antarctic Logistics and Operations"
Rome, Italy, Aug. 1994
and can be found in the Symposium's Proceedings, p 97-105.

Please direct any query about the paper either to
Hervé LeGoff / Uli Hasert, Email: legoff@ensic.u-nancy.fr, or Fax: +33 3 83 32 29 75, or to
Antoine Guichard, Email: antoine.guichard@latitude.aq, or Fax: +61 3 6229 1441
an electronic copy of this paper is available at www.latitude.aq
